Available online at www.sciencedirect.com

ScienceDirect

IFAC Papers Online CONFERENCE PAPER ARCHIVE

IFAC PapersOnLine 54-17 (2021) 81–86

Hyperchaos from DTC Induction Motor Drive System

Ahmed S. Hunaish[1]. Fadhil R. Tahir[2]. Hamzah A Abbood[3]

[1]Basrah Oil Company, Basrah, Iraq
[1] Electrical Engineering Department, University of Basrah, Basrah, Iraq
(Tel: 00964 770 5709 214; e-mail: ahm782013@qmail.com).
[2]Electrical Engineering Department, University of Basrah,
Basrah, Iraq, (e-mail: fadhilrahma.creative@gmail.com)
[3]PetroChina International Iraq FZE Iraq Branch, Production Department,
Maysan, Iraq, (e-mail: hamza.abd.k@gmail.com)

Abstract: In the present work, a 3-phase induction machine model has been derived in a stationary-reference-frame. The strategy of the direct torque control (DTC) with a constant voltage-to-frequency ratio is used to control the obtained model. The obtained driven machine system involves nine nonlinear first-order differential equalities. The nine-dimensional system performance is investigated by using the numerical analysis due to changes in the parameter of the control part. The gain of the integral in the speed part of the controller is designated to investigate the dynamics of the modeled system. The results illustrate that the system has a period-doubling (period-1, period-2, and period-4) bifurcation route to chaotic oscillation. The bifurcation diagram and Lyapunov exponent spectrum assign these situations. Period-5 is noted in a window inside the bifurcation diagram. The large positive magnitudes of two of Lyapunov exponents show that the system is hyperchaos, which denotes the system shows very strong randomness and a high degree of disturbance. The system generates different coexisting attractors (periodic and chaotic attractors) for different values of the integral gain of the speed control loop.

Keywords: Hyperchaos, bifurcation, chaos, coexisting attractors, direct torque control.

1. INTRODUCTION

Nowadays, the nonlinear behaviors of systems are studied essential in nearly every domain of sciences. The nonlinear systems can display a large diversity of behaviors produce the response solution hard to find in several states, even at what time numerical approaches are existing (Rugonyi and Bathe, 2003). It is now a prevalent trust that conception and employment of the substantial dynamics, such as bifurcations and chaotic states, of nonlinear systems have a significant influence on the modern technologies. Dynamic system behaviors such chaos have been studied in many sections of engineering. Also, chaotic phenomena and its employment in machine drive systems were excessively put out as published articles (K. T.Chua and Zheng Wang, 2011).

In electrical drives, there are many studies related to bifurcation and chaos behaviors. In (Chau et al., 1997; Chau, K. T., Chen, J. H., Chan , C. C., Pong, J. K. H., & Chan, 1997), validation was done by comparing bifurcation diagram points in PSpice simulation with the obtained period-1, period-p and chaotic cases of the DC drive system prototype. In (Bhattacharya and Mandal, 2017), the 2nd order generalized reiterated charts that depict the nonlinear dynamics of both current and voltage methods controlled DC machine drive systems over the continuous conduction operation mode were illustrated; the computer simulation showed that the system displays more than one type of bifurcation caused by the system parameters change. Gao et al. showed that the Hopf bifurcation and chaos appear in the permanent-magnet synchronous machine dynamics; the theoretical analysis has been verified by the experimental result (Gao, Y and Chau, 2003). Gao et al. proved that Hopf bifurcation (HB) and chaos cases exist in the synchronous reluctance machine (SynRM) drive system by using theoretical analysis and simulations then validated experimentally (Y. Gao and K. T. Chua, 2004). In the paper (Lu, Li and Li, 2009), the HB criterion for an induction motor drive system was obtained for different parameters as stator and rotor resistances as well as the inertial constant. Sangrody et al. concentrated onto analyze chaotic and bifurcation responses related to the induction motor (IM) scalar drives with a modified Poincare's map; they found that the change in the proportional gain of the speed controller for different speed commands can lead to chaotic or stable responses (Sangrody, Nazarzadeh and Nikravesh, 2012). Jain et al. used a numerical analysis of many types of bifurcations for proportional-integral-controlled indirect vector-controlled induction motor (IVCIM); simulation and experimental outcomes are viewed to validate the bifurcation behaviors (Jain and Ghosh, S., & Maity, 2018). In the paper (Ghosh, Panda and Saha, 2018), in the case of the impact commutation-phenomenon and slotting effect, some notable nonlinear behaviors were noticed. The simulation results for a nonlinear IM drive system consists of the ninth-order show the system bifurcates to a period-doubling route to chaos (Hunaish and Tahir, 2020). The nonlinear dynamics of an eighth-order 3-phases IM drive system with an indirect field-

10.1016/j.ifacol.2021.11.029

oriented controller (IFOC) has been used where the system shows periodic and chaotic bifurcation as well as coexisting attractors (Hunaish and Tahir, 2021a, b).

The coexisting attractors in the dynamics of the nonlinear systems had also more interesting during the last years. Many studies were established for different nonlinear systems: Lai et al. introduced a bifurcation diagram, Lyapunov spectrum, and phase portrait to state the existence of multiple chaotic and coexisting attractors in the Sprott B system by using theoretical and numerical analysis (Lai and Chen, 2016). Lai et al. analyzed the system equilibrium points and used the numerical simulation method to indicate that the used system reveals pairs of point, periodic, and strange attractors with the parameter of the system variation; an electronic circuit was also considered to check the chaotic states of the modelled system (Lai et al., 2018). Lai et al. found coexisting attractors for an extended Lü system which are presented by the bifurcation diagrams and Lyapunov exponent spectrum; they designed an electronic circuit for showing the coexistence of chaotic attractors (Lai, Norouzi and Liu, 2018). In (Singh, Roy and Kuznetsov, 2019), the PMSM dynamics is investigated to state the multi-stability, hidden-attractors, and coexisting attractors in its dynamics. A simple chaotic system has five terms with two nonlinearities was used to show the appearance of infinite coexisting chaotic attractors (Lai et al., 2019).

All the above electric drive dynamic studies related to DC, permanent-magnet synchronous machine, SynRM, and IM drive systems. The induction motor drives have key role in industrial applications, spatially the direct torque control (DTC). The dynamics behavior (bifurcations and chaos) of DTC drive system for IM as well as hyperchaos were not mentioned in the previous literatures. This motivated us to investigate its dynamics.

In this paper, the IM with DTC drive system is used to analyze the dynamics of the systems due to the variation of the PI speed loop parameters. Period-doubling bifurcation route to chaos, period-1, period-2, period- 4, period-5 and chaos are achieved by using computer simulation. The hyperchaos in the system dynamics is shown by Lyapunov exponent spectrum. The coexisting attractors are stated in the phase portrait figures.

The rest of paper is divided into three sections: Section 2 deals with DTC IM system modeling. The scheme of the DTC IM system is introduced and a DTC model is derived mathematically to investigate the system dynamics. The obtained DTC model consists of nine nonlinear first-order differential equations. Section 3 includes the dynamical analysis of the system. The bifurcation diagram of the speed of the motor supported with Lyaponuv exponent spectrum for a certain range of PI speed integral gain are plotted by using computer simulation to reveal the period-doubling route to chaos. The hyperchaos is indicated in the Lyaponuv exponent spectrum and the coexisting attractors are also noted. Finally, conclusion is provided in Section 4.

2.MODEL OF DTC IM DRIVE SYSTEM

DTC technique adopts vector states of output voltage based on the torque and stator flux magnitude errors by using space vector modulation (SVM) method without current loops (Bose, 2001). In this section, the IM model and the overall IM drive model with DTC have been obtained.

The general stationary d-q model of a squirrel-cage IM can be stated according to (Ong, 1998), to have the following IM dynamic system:

$$\dot{\lambda}^{s}_{qs} = -R_s\left[\frac{L_r}{L_sL_r - L_m^2}\lambda^{s}_{qs} - \frac{L_m}{L_sL_r - L_m^2}\lambda^{s'}_{qr}\right] + v^{s}_{qs} \quad (1)$$

$$\dot{\lambda}^{s}_{ds} = -R_s\left[\frac{L_r}{L_sL_r - L_m^2}\lambda^{s}_{ds} - \frac{L_m}{L_sL_r - L_m^2}\lambda^{s'}_{dr}\right] + v^{s}_{ds} \quad (2)$$

$$\dot{\lambda}^{s'}_{qr} = -R'_r\left[-\frac{L_m}{L_sL_r - L_m^2}\lambda^{s}_{qs} + \frac{L_s}{L_sL_r - L_m^2}\lambda^{s'}_{qr}\right] + \omega_r \quad (3)$$

$$\dot{\lambda}^{s'}_{dr} = -R'_r\left[-\frac{L_m}{L_sL_r - L_m^2}\lambda^{s}_{ds} + \frac{L_s}{L_sL_r - L_m^2}\lambda^{s'}_{dr}\right] - \omega_r\lambda^{s'}_{qr} \quad (4)$$

$$\dot{\omega}_r = \frac{p}{2J}\left[\frac{3p}{4}\frac{L_m}{L_sL_r - L_m^2}\left(\lambda^{s}_{qs}\lambda^{s'}_{dr} - \lambda^{s}_{ds}\lambda^{s'}_{qr}\right) - T_l\right] \quad (5)$$

where: λ^{s}_{qs}, λ^{s}_{ds}, $\lambda^{s'}_{qr}$, $\lambda^{s'}_{dr}$, v^{s}_{qs}, and v^{s}_{ds} are the stator and rotor fluxes, stator voltages in quadrature and direct axis referred to stator, respectively, and ω_r is the rotor speed. The system parameters are defined in Table 1.

The DTC scheme with constant voltage-to-frequency ratio is shown in Fig. 1. The controller outputs are the magnitude and angle of the voltage of the motor stator. According to these outputs, the space vector modulation is designed and applied to the three phase inverter which supplies the three phase induction motor.

Table 1. System parameters definition

Parameter	Definition	Parameter	Definition
R_s	Stator resistance	p	Number of poles
L_s	Stator inductance	T_l	Load torque
R'_r	Rotor resistance	k_{ps} and k_{is}	Speed PI gains
L_r	Rotor inductance	k_{pT} and k_{iT}	Torque PI gains
L_m	Mutual inductance	k_{pf} and k_{if}	Flux PI gains
J	Rotor inertia	λ^{*}_{s}	The stator reference flux

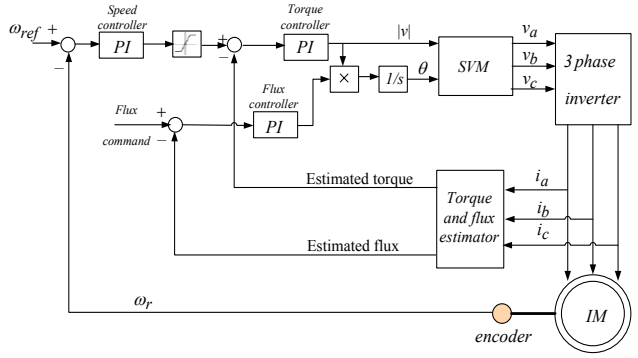

Fig. 1. DTC drive system scheme.

Table 2. IM parameters

Parameter	Value	Parameter	Value
Nominal voltage (V)	220	Stator inductance (mH)	43.9
Supply frequency (Hz)	50	Rotor resistance (Ω)	3
Rated speed (rpm)	1430	Rotor inductance (mH)	43.9
Number of poles	4	Mutual inductance (mH)	278
Stator resistance (Ω)	3.3	Rotor inertia (kgm²)	0.00665

By defining nine state variables, $x_1 = \lambda_{qs}^s$, $x_2 = \lambda_{ds}^s$, $x_3 = \lambda_{qr}^{s'}$, $x_4 = \lambda_{dr}^{s'}$, $x_5 = \omega_r$, $x_6 = \left(k_{ps} + k_{is}\int dt\right)\left(\omega_{ref} - \omega_r\right)$, $x_7 = \left(k_{pT} + k_{iT}\int dt\right)\left(T_e^* - \hat{T}_e\right)$, $x_8 = \left(k_{pf} + k_{if}\int dt\right)\left(\lambda_s^* - \hat{\lambda}_s\right)$, and $x_9 = \theta$, the DTC model can be given as following:

$$\dot{x}_1 = -R_s\left[c_1 x_1 - c_2 x_3\right] + v_{qs}^s \tag{6}$$

$$\dot{x}_2 = -R_s\left[c_1 x_2 - c_2 x_4\right] + v_{ds}^s \tag{7}$$

$$\dot{x}_3 = R_r'\left[c_2 x_1 - c_3 x_3\right] + x_4 x_5 \tag{8}$$

$$\dot{x}_4 = R_r'\left[c_2 x_2 - c_3 x_4\right] - x_3 x_5 \tag{9}$$

$$\dot{x}_5 = \frac{p}{2J}\left[\frac{3p}{4}c_2\left(x_1 x_4 - x_2 x_3\right) - T_l\right] \tag{10}$$

$$\dot{x}_6 = -\frac{k_{ps}\,p}{2J}\left[\frac{3p}{4}c_2\left(x_1 x_4 - x_2 x_3\right) - T_l\right] + k_{is}\left(\omega_{ref} - x_5\right) \tag{11}$$

$$\dot{x}_7 = k_{pT}\left(\dot{x}_6 - \frac{3p}{4}c_2\left(\dot{x}_4 x_1 - x_3 \dot{x}_2 - x_2 \dot{x}_3 + x_1 \dot{x}_4\right)\right) + k_{iT}\left(x_6 - \frac{3p}{4}c_2\left(x_1 x_4 - x_2 x_3\right)\right) \tag{12}$$

$$\dot{x}_8 = k_{if}\left(\lambda_s^* - \sqrt{x_1^2 + x_2^2}\right) - k_{pf}\frac{x_1 + x_2}{\sqrt{x_1^2 + x_2^2}} \tag{13}$$

$$\dot{x}_9 = x_7 x_8 \tag{14}$$

where $c_1 = \dfrac{L_r}{L_s L_r - L_m^2}$, $c_2 = \dfrac{L_m}{L_s L_r - L_m^2}$, and $c_3 = \dfrac{L_s}{L_s L_r - L_m^2}$

3. DYNAMICAL ANALYSIS

The nonlinear dynamical system through (6)-(14), gives the bifurcation occurrence with the variation of the system parameter. In fact, numerical analysis is helpful for higher order dynamic systems where mathematical analysis perhaps is not efficient. The familiar tools that are used to investigate the system dynamics are the bifurcation diagram and Lyapunov exponent spectrum.

The motor parameters are listed in Table 2 (Zhang, Chau and Wang, 2012). The controller parameters are set to: $k_{pf} = k_{if} = 0.01$, $k_{pT} = k_{iT} = 1$, $k_{ps} = 0.001$. It is noted that k_{is} is selected as the bifurcation parameter.

The reference speed ω_{ref} is set to 314 rad/sec at no load and the reference flux is determined approximately from magnitude of motor voltage |*v*| and the voltage frequency *f* as following (Pimkumwong and Wang, 2018):

$$\lambda_s^* = \frac{|v|}{2\pi f} \tag{15}$$

Fig. 2(a) illustrates the IM speed bifurcation diagram due to k_{is} changes and Fig. 2(b) is the corresponding Lyapunov exponent spectrum. From Fig. 2(a) one can note that for the range of $k_{is} \in$ (20,91.3), the system operates normally where the motor speed tracks the command speed (stable fixed point). A stable periodic solution is occurred (period-1) at k_{is}=91.4, at window from 137.3 to 138.4, and at window from 168.4 to 171.8, also period doubling is appeared as period-2 at k_{is}=105.4 and at window from 160 to 163.9. Period-4 is noted at k_{is}=108.4. While period-5 can be seen clearly for k_{is} from 111.3 to 111.5. The period-4 leads to the route to non-periodic solution (chaos), the chaos speed is appeared at k_{is}=109 while some windows have stable limit cycles as mentioned recently.

The Lyapunov exponent spectrum has been obtained to emphasis the bifurcation diagram result, Fig. 2(b), depicts the Lyapunov exponent spectrum. From Fig. 2(b), the system gives chaotic oscillations at k_{is} =109. It is noted that the system is hyperchaos. Where the hyperchaotic dynamics is defined mathematically as a chaotic system with more than one positive Lyapunov exponent including that system dynamics are expended in many various directions concurrently; thus, in hyperchaos, dynamic system behaviors are more complex (Vaidyanathan et al., 2015). It is clear that the DTC drive system has two large positive exponents, which implies the system exhibits very strong randomness and a high degree of chaos.

The time response and phase portrait which represent the chaos case are shown in Fig. 3(a) and (b) respectively. In Fig. 3, when k_{is} is 250, the motor speed oscillates in hyperchaotic manner with very large number of waves which differ in amplitude and oscillation size.

The following test is relevant to show sensitivity of the steady state response to the variation in the initial values of variables. In Fig. 4 and Fig. 5, the coexisting attractors can be seen for different initial values (X(0) = ($x_1(0)$, $x_2(0)$, $x_3(0)$, $x_4(0)$, $x_5(0)$, $x_6(0)$, $x_7(0)$, $x_8(0)$, $x_9(0)$). Fig. 4, for k_{is} =125.1, shows different coexisting attractors. Period-2 attractor is shown in Fig. 4(a) from initial value (0,0,0,0,50,0,0,0,0) and chaotic attractor is illustrated in Fig. 4(b) from initial value (0.3, -0.3, 0.3, -0.3, 150, 0, 0, 0, 0). Fig. 5 shows a state in which a period-1 attractor exists with a chaotic attractor. Period-1 attractor appears from X(0)= (0, 0, 0, 0, 50, 0, 0, 0, 0) and the chaotic attractor from X(0) = (0.2, -0.1, 0.1,- 0.1, 100, 0, 0, 0, 0) as shown in Fig. 5.

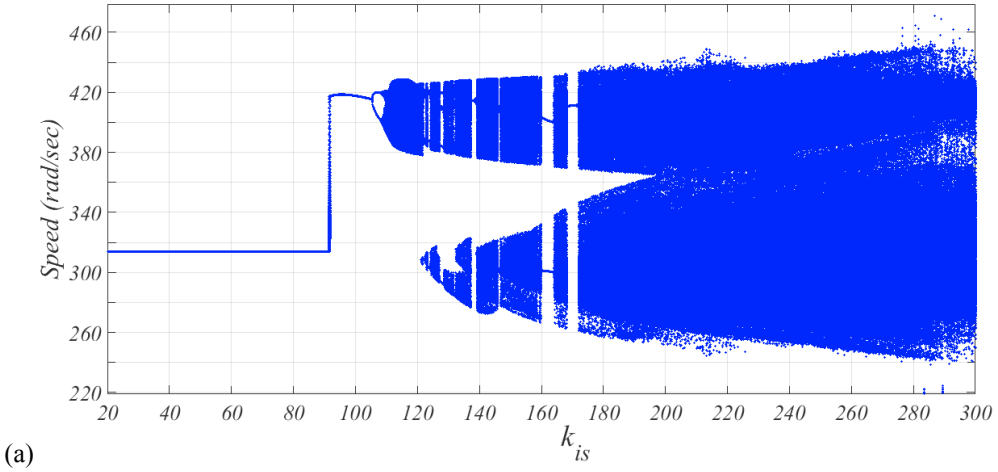

(a)

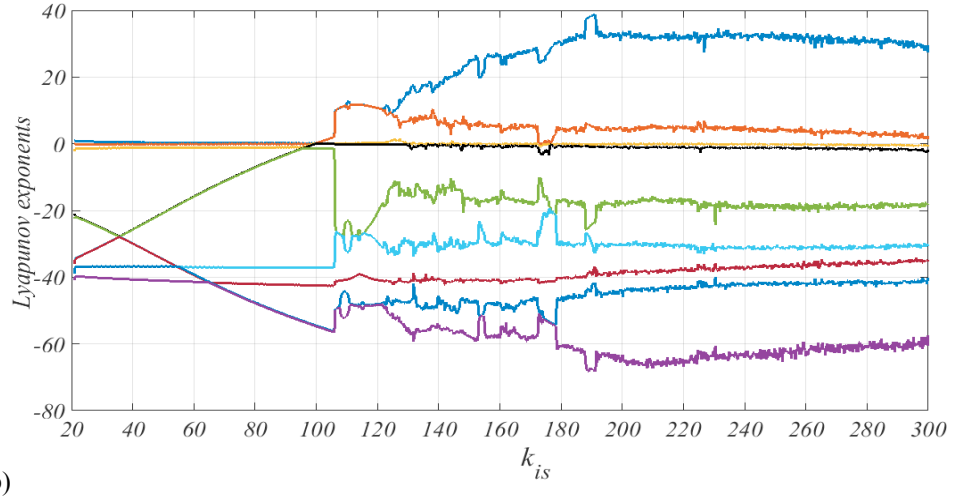

(b)

Fig. 2. DTC IM drive system dynamics: (a) Bifurcation diagram; (b) Lyapunov exponent spectrum.

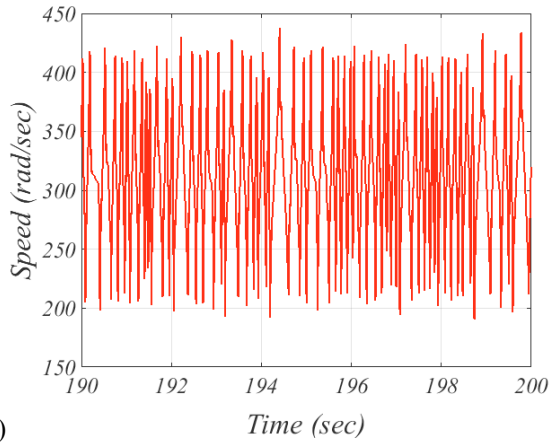

(a)

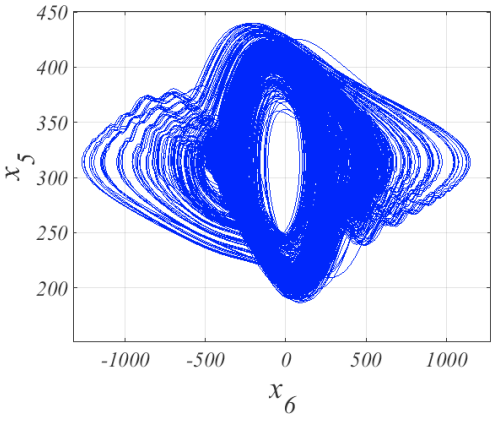

(b)

Fig. 3. (a) Time response of motor speed; (b) phase portrait. Both with $k_{is} = 250$.

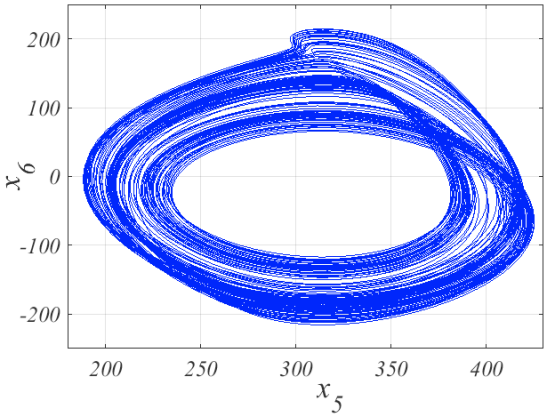

(a)

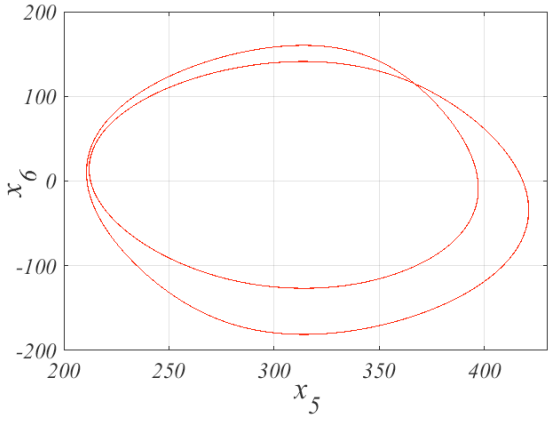

(b)

Fig. 4. Phase portrait with $k_{is} = 125.1$: (a) period-2 from initial value (0,0,0,0,50,0,0,0,0); (b) chaos from initial value (0.3,-0.3,0.3,-0.3,150,0,0,0,0).

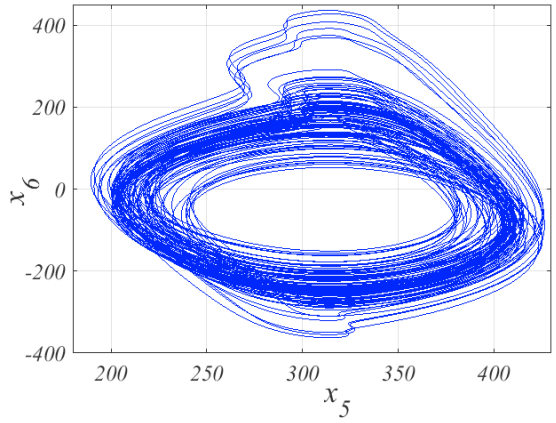

(a)

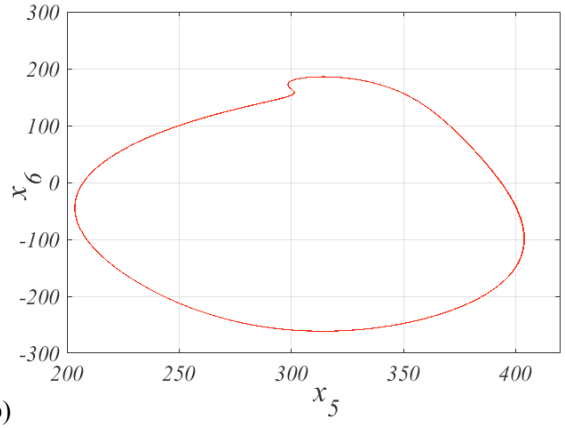

(b)

Fig. 5. Phase portrait with $k_{is} = 159.9$: (a) period-1 from initial value (0,0,0,0,50,0,0,0,0); (b)chaos from initial value (0.2,-0.1,0.1,-0.1,100,0,0,0,0)

4. CONCLUSIONS

The mathematical model of a 3-phase induction machine has been obtained in a stationary-reference-frame which is controlled by using a direct torque control technique with a constant voltage-to-frequency ratio. The dynamical behavior of the nine-dimensional system has been investigated due to the change in the control parameter based on the numerical analysis. The gain variation of the integral part of the speed controller has been selected to show the dynamical system response. The obtained results state that the motor drive

system has period-1, -2, and -4, bifurcation then the system to be chaotic oscillation, the bifurcation diagram and Lyapunov exponent spectrum assigned these situations. Period -5 is indicated in a window inside the bifurcation diagram. The two large positive Lyapunov exponents show that the system is hyperchaotic, therefore; this is reflected as a very strong chaotic oscillation in the motor speed. These results indicate that the system dynamic complexity increased with the increase of the integral speed gain. The coexisting attractors are indicated for specific values of integral gain with different initial values. In future work, a controller will be designed to suppress the chaotic behavior. REFERENCES

Bhattacharya, S. and Mandal, S. K. (2017). Analysis of switching loss in chaotic and non-chaotic state of pmdc drive. 2*016 International Conference on Computer, Electrical and Communication Engineering, ICCECE 2016*, pp. 7–10.

Bose, B. K. (2001). *Modern power electronics and ac drives,* ch8. Prentice Hall PTR, USA.

Chau, K. T. et al. (1997). Chaotic behavior in a simple dc drive. *in Proceedings of Second International Conference on Power Electronics and Drive Systems*, pp. 523–528.

Chau, K. T. et al. (1997). Modeling of subharmonics and chaos in dc motor drives. *in Proceedings of the IECON'97 23rd International Conference on Industrial Electronics, Control, and Instrumentation (Cat. No.97CH36066)*, pp. 523–528.

Gao, Y and Chau, K. T. (2003). Design of permanent magnets to avoid chaos in pm synchronous machines. *IEEE Transactions on Magnetics*, 39(5), pp. 2995–2997.

Ghosh, M., Panda, G. K. and Saha, P. K. (2018). Analysis of chaos and bifurcation due to slotting effect and commutation in a current discontinuous permanent magnet brushed dc motor drive. *IEEE Transactions on Industrial Electronics*, 65(3), pp. 2001–2008.

Hunaish, A. S. and Tahir, F. R. (2020). Bifurcation and chaos from dtc induction motor drive system. *IJEEE* , 16(1), pp. 1–5.

Hunaish, A. S. and Tahir, F. R. (2021a). Bifurcation and chaos in indirect field-oriented controlled induction motor drive system. *European Physical Journal Plus*, 136(4), pp. 1-13.

Hunaish, A. S. and Tahir, F. R. (2021b). Fixed-time synergetic control-based chaos suppression for eighth-order ifocim drive system. *International Journal of Bifurcation and Chaos,*31(9), 2150131.

Jain, J. K.., Ghosh, S., and Maity, S. (2018). A numerical bifurcation analysis of indirect vector-controlled induction motor. *IEEE Transactions on Control Systems Technology*, 26(1), pp. 282–290.

K. T.Chua and Zheng Wang (2011). *Choas in electric drive systems: analysis, control and application*. First Edit, John Wiley & Sons (Asia), Singapore.

Lai, Q. et al. (2018). A new chaotic system with multiple attractors: dynamic analysis, circuit realization and s-box design. *Entropy*, 20(1), pp. 1–15.

Lai, Q. et al. (2019). An extremely simple chaotic system with infinitely many coexisting attractors. *IEEE Transactions on Circuits and Systems II: Express Briefs*, PP(1), pp. 1–1.

Lai, Q. and Chen, S. (2016). Generating multiple chaotic attractors from Sprott b system. *International Journal of Bifurcation and Chaos*, 26(11), pp. 1–13.

Lai, Q., Norouzi, B. and Liu, F. (2018). Dynamic analysis, circuit realization, control design and image encryption application of an extended Lü system with coexisting attractors. *Chaos, Solitons and Fractals*, 114, pp. 230–245.

Lu, Y., Li, H. and Li, W. (2009). Hopf bifurcation and its control in an induction motor system with indirect field oriented control. *in 2009 4th IEEE Conference on Industrial Electronics and Applications, ICIEA 2009*, pp. 3438–3441.

Ong, C.-M. (1998). *Dynamic simulation of electric machinery using matlab /simulink*, ch6. Prentice Hall PTR, USA.

Pimkumwong, N. and Wang, M. S. (2018). Full-order observer for direct torque control of induction motor based on constant v/f control technique. *ISA Transactions*, 73, pp. 189–200.

Rugonyi, S. and Bathe, K. J. (2003). An evaluation of the Lyapunov characteristics exponent of chaotic continuous systems. *International Journal for Numerical Methods in Engineering*, 56(1), pp. 145–163.

Sangrody, R. A., Nazarzadeh, J. and Nikravesh, K. Y. (2012). Bifurcation and Lyapunov's exponents characteristics of electrical scalar drive systems. *IET Power Electronics*, 5(7), pp. 1236–1244.

Singh, J. P., Roy, B. K. and Kuznetsov, N. V. (2019). Multistability and hidden attractors in the dynamics of permanent magnet synchronous motor. *International Journal of Bifurcation and Chaos*, 29(4), pp. 1–17.

Vaidyanathan, S. et al. (2015). Design and SPICE implementation of a 12-term novel hyperchaotic system and its synchronisation via active control. *International Journal of Modelling, Identification and Control*, 23(3), pp. 267–277.

Y. Gao and K. T. Chua (2004). Hopf bifurcation and chaos in synchronous reluctance motor drives. *IEEE Transactions on Energy Conversion*, 19(2), pp. 296–302.

Zhang, Z., Chau, K. T. and Wang, Z. (2012). Chaotic speed synchronization control of multiple induction motors using stator flux regulation. *IEEE Transactions on Magnetics*, 48(11), pp. 4487–4490.